Computer Assisted Mechanics and Engineering Sciences, 5: 299–309, 1998.

Some remarks on the applicability of rectangular elements to plane strain boundary value problems

Andrzej Jarzębowski and Jan Maciejewski
Institute of Fundamental Technological Research Polish Academy of Sciences
Świętokrzyska 21, 00-049 Warsaw

(Received August 4, 1997)

The aim of this paper is the discussion on the applicability of some rectangular elements to plane strain boundary value problems. Four different elements were considered: 4-node, 5-node, Serendipity 8-node and Lagrangian 9-node. Two cases: the material layer loaded by a concentrated vertical force and the same layer loaded by a symmetrical rigid punch were discussed. An elastic material was used to avoid the influence of the constitutive model on solutions. To model interface behaviour on the contact surface a Coulomb friction condition was applied. The use of the 4- and 5-node elements resulted in the prediction of the "island" pattern of stress and strain tensors distributions and their non-applicability was proved independently from the boundary condition. The 8-node element predicted erroneous distributions of nodal forces and should be avoided in the case of contact problems. Among the discussed group of elements only the 9-node element turned out to be applicable for boundary value problems under plane strain condition.

1. Introduction

One of the major problems faced by a Finite Element Method user, who wants to develop his own computer code, is the problem of a proper selection of a finite element to be applied. This choice must be done according to a type of a boundary value problem which has to be solved. Usually, a less experienced person uses one from a huge amount of numerical methods handbooks to search for an advice. Unfortunately, very often there is no proper one, especially for plane strain problems. As we know, there are no plane problems in mechanics of continua; instead, there are only plane strain and plane stress problems in two dimensional cases. The former ones are the subject of this study. The problems which are going to be reported in this paper raised up during authors study of the soil compaction phenomena using a model of the static road roller with a rigid cylinder. Series of original experiments were conducted in semi-laboratory scale using the special apparatus allowing for recording of the soil deformation through a transparent wall. Then tests were simulated using FEM code with the modified Infinite Number of Surfaces Model, developed for non-cohesive soils by Jarzębowski and Mróz [1], allowing for the proper description of material hardening and softening accompanied by the compaction and the dilatancy of soil for a monotonic and cyclic loading in the initial and advanced stages of the elasto-plastic deformation. Experiments were simulated in two stages: putting the cylinder on the soil surface and subsequent rolling . Both stages were executed using small steps. As a consequence a solution of boundary value problem with a changing number of contact nodes was predicted. Especially in the rolling stage new nodes became into contact in the front area of the cylinder whereas some nodes separated in the area behind the cylinder. A Coulomb friction condition was applied to model interface behaviour on the rigid punch-material layer contact surface. There are no, so called, "interface elements" used in this study. The friction condition was checked in every contact node. A plane strain condition was assumed according to the experimental laboratory condition. A very good coincidence of experimental and predicted results (for 9-node element with 3 x 3 integration points) was obtained for various traction parameters of the rolling process. The comparison of results was a subject of another paper [2].

However, during the numerical simulation of the considered boundary value problems using other rectangular elements peculiar stress, strain and nodal forces distributions were observed. In Fig. 1a the horizontal stress distribution for 4-node element is presented, showing "island like pattern". For the 8-node element peculiar nodal force distribution was observed (Fig. 1b).

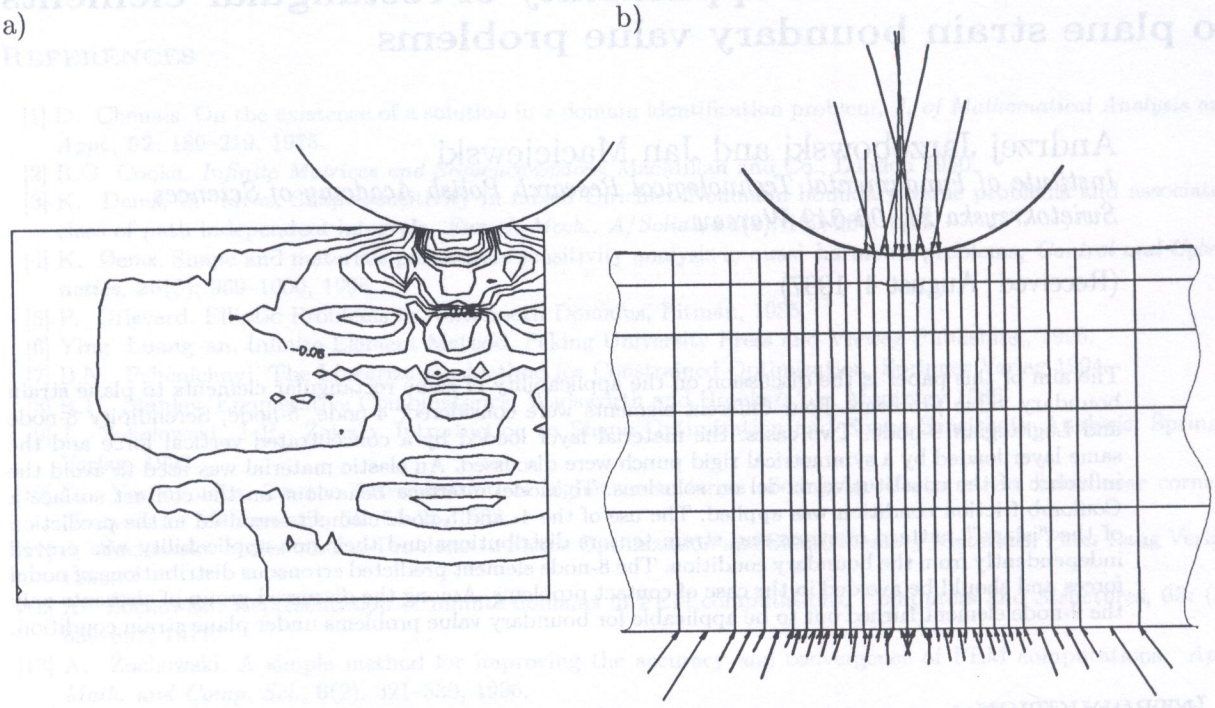

Fig. 1. Simulation of the compaction process under the rigid cylinder; a) horizontal stress distribution using the 4-node element, b) nodal force distribution using the 8-node element

If one considers the material of the layer to be the elasto-plastic one, modelled by any advanced constitutive model, which obeys the influence of stress history on the evolution of material parameters (like the INS model), the essential for the whole solution will be the proper prediction of stress and strain distributions within the whole layer for any calculation step, and distributions similar to those presented in Fig. 1a are unacceptable. In order to investigate the applicability of rectangular elements simple boundary value problems using concentrated loading force and a rigid punch were simulated. To avoid the influence of a type of constitutive elasto-plastic model on the major features of the problem discussed, only elastic properties of the layer are assumed in this study.

Consider a layer of a finite thickness h and finite length l, supported by a rigid sub-base (Fig. 2). Let us assume a constant width w of the layer, perpendicular to the plane of the figure. As the width w does not change during the deformation process we obtain a plane strain problem. Assume, that the layer is centrally loaded by a concentrated vertical force and four different boundary conditions are considered (Fig. 2a-d). Subsequently, consider the same layer to be loaded by a symmetrical rigid punch of various width w (Fig. 3).

Let us assume, that the elastic properties are described by a pair of constants, for example bulk and shear moduli, denoted by K and G, respectively ($K = E/3(1-\nu), G = E/2(1+\nu)$, where E and ν denote the Young modulus and the Poison's ratio). Although the material behaviour is assumed to be linear, each solution was obtained in several steps, because of the contact condition applied on the material layer-punch interface.

Four different rectangular elements were applied: 4-node, 5-node, Serendipity 8-node and Lagrangian 9-node (Fig.4). Precise descriptions of 4-node, 8-node and 9-node elements were given by Hinton & Owen [3; pp. 245-251], Zienkiewicz & Taylor [4] and Oden & Reddy [5]. The 5-node

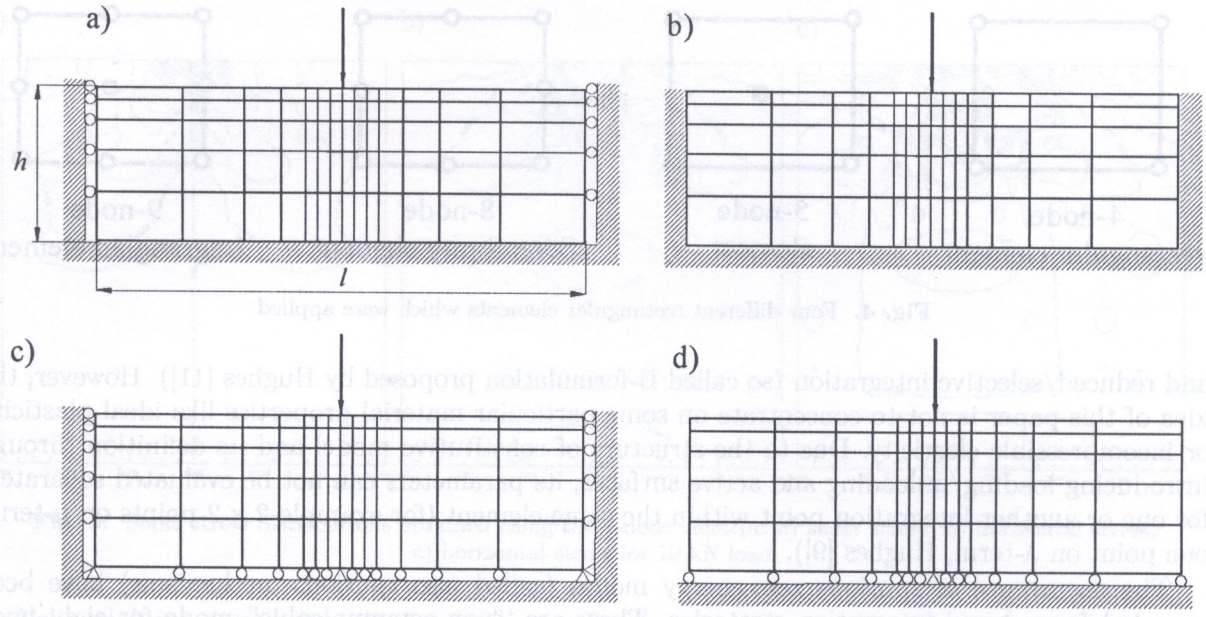

Fig. 2. Four different boundary conditions of the considered layer

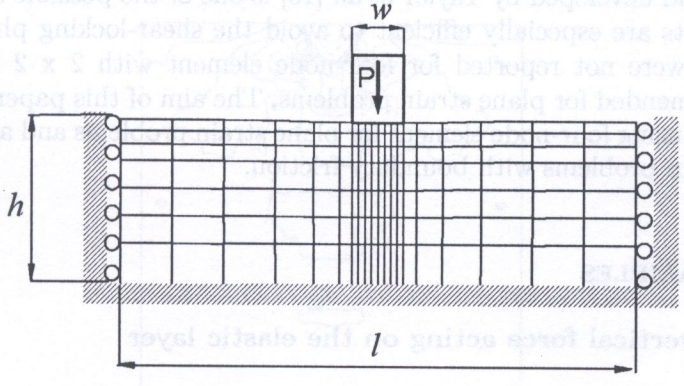

Fig. 3. The layer loaded by a symmetrical rigid punch

element was developed as a simplification of the 9-node Lagrangian element. It was assumed, that the motion of midside points is a mean value of motion obtained for the corner nodes.

There are several papers concerning the applicability of various elements for some specific elasto-plastic problems [6–9]. Among other subjects, a proper prediction of collapse loads for the rigid punch penetration problem for various types of elements was discussed by Sloan and Randolph [6]. However, only the perfectly smooth punch surface was concerned and the incompressible, additionally constrained, elasto-plastic material was used in this study.

The well known effect of element locking (for isochoric plastic flow) was discussed by de Borst and Groen [10] for dilating and contracting soils basing on the simple form of dilatancy equation. In fact, for the ideal plasticity governed by such an equation with the constant dilatancy angle the effect of element locking is expected for patch test for conventional 4-node element. However, it should not occur for an advanced elasto-plastic model with the developing plasticity [1] (from pure elastic behaviour to fully elasto-plastic) and certainly not for pure elasticity (excluding incompressible case). Thus, the authors did not suspect the effect of element locking to be responsible for the phenomena reported in this paper.

It is worth mentioning that several methods have been developed to avoid such a disadvantage of four node element, as the above described element locking. The best known are mixed approaches

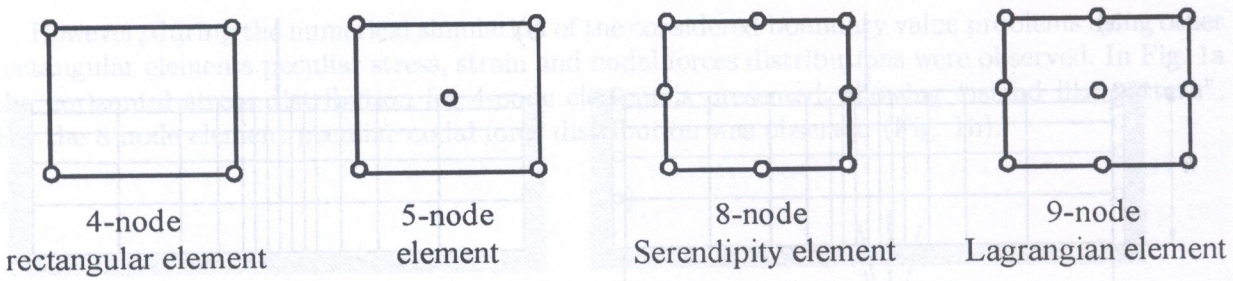

Fig. 4. Four different rectangular elements which were applied

and reduced/selective integration (so called B-formulation proposed by Hughes [11]). However, the idea of this paper is not to concentrate on some particular material properties like ideal plasticity or incompressible elasticity. Due to the structure of constitutive model and its definition through introducing loading/unloading and active surfaces, its parameters can not be evaluated separately for one or another integration point within the same element (for example 2 x 2 points on μ-term, one point on λ-term, Hughes [9]).

The occurrence of spurious zero-energy modes (called also spurious mechanisms) have been reported for reduced integration strategies. These are, "non-communicable" mode for eight-node serendipity quadrilateral element with 2 x 2 quadrature and "hour-glass" mode for two-dimensional bilinear element with one point Gauss rule [8]. The application of incompatible modes, proposed by Wilson et al. [12] and developed by Taylor et al. [13] is one of the possible solutions in the latter case [9]. Those concepts are especially efficient to avoid the shear-locking phenomenon. However, spurious mechanisms were not reported for four-node element with 2 x 2 Gaussian integration which is widely recommended for plane strain problems. The aim of this paper is to argue, that one should generally avoid using four-node element for plane strain problems and avoid using eight-node element for plane strain problems with boundary friction.

2. Numerical examples

2.1. Concentrated vertical force acting on the elastic layer

2.1.1. 4-node element

Assume that the layer described in Sec. 1 under the boundary condition illustrated in Fig. 2a. was loaded by a concentrated vertical force increasing from 0 to the final value of 4000 N. Let us solve that problem using the 90 node mesh assembled of 70 4-node rectangular elements. At the beginning the 2 x 2 integration rule was applied.

The predicted solution was satisfactory in the case of boundary values such as nodal displacements and nodal forces. Unfortunately, the situation changes if one would investigate carefully distributions of all components of stresses and strains within the sample. Some distributions, such as shear stress σ_{xy} (Fig. 5a) were reasonable too, but some other, like horizontal stress σ_x distribution (Fig. 5b) showed non-physical layered structure, corresponding to the structure of the mesh applied. The effect of layered pattern would develop if one continues the loading process. The horizontal stress σ_x distribution for vertical force equal to 10 kN was shown in Fig. 5c. The characteristic "island" layered pattern is well visible. Thus, from the physical point of view this solution has to be excluded.

To exclude the influence of the boundary condition on the layered pattern development three different conditions were considered (Fig. 2b-d). However, similar solutions were obtained. For more precise investigation of this phenomenon additional calculations were performed using more precise mesh discretization. The 7 by 20 elements mesh was used, but it did not influence the layered structure of the solution at all.

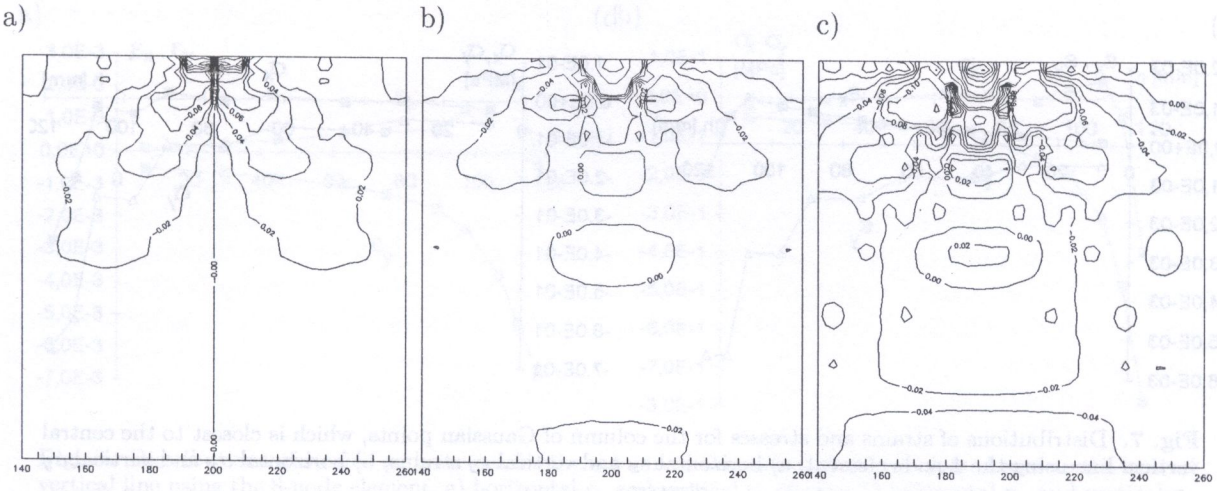

Fig. 5. Some stress distributions obtained using the 4-node element: a) shear stress, b) horizontal stress, c) horizontal stress for 10 kN load

Next trial was done using nine integration points in every element (3 x 3). As it can be seen in Fig.6, the change of the number of Gaussian points from 4 to 9 do not influence the solution very much and "island" layered pattern is still well visible. Let us try to explain the phenomenon of the

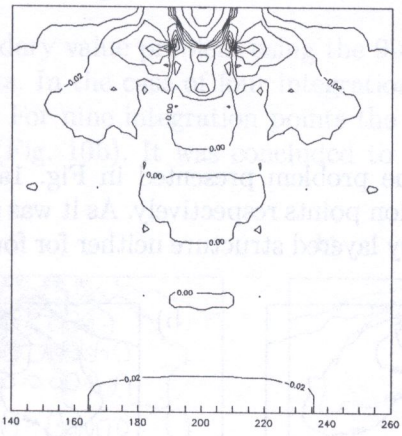

Fig. 6. Horizontal stress distribution for the 4-node element and nine integration points

layered structure development in the case of the four-node element with four integration points. In every calculation step the nodal displacement field is obtained and strain distributions calculated. It is a feature of the four node element, that vertical strain is constant along the vertical direction within every layer of elements for every particular column of Gaussian points. Distributions of horizontal ε_x and vertical ε_y strains for the column of Gaussian points, which is closest to the central vertical line were plotted in Fig. 7a. Thus, the combination of slightly increasing horizontal strain ε_x and decreasing vertical strain ε_y (from layer to layer) generates oscillatory distributions of stresses in the considered column of Gaussian points. Those distributions were shown in Fig. 7b. The effect of layered structure of the solution was obtained independently from the set of elastic constants, which were used during the calculation. Three different layers were independently simulated (in separate calculations) and three sets of constants were applied for this reason. They correspond to elastic properties of three different geological materials: dense sand ($\nu = 0.25, E = 120$ MPa), plastic clay ($\nu = 0.35, E = 15$ MPa) and cohesive soil ($\nu = 0.45, E = 25$ MPa). Those constants were measured for the reloading stress path, for which material obeys elastic behaviour. All obtained distributions were similar. Although one may imagine, that a material with very low value of Poison's ratio

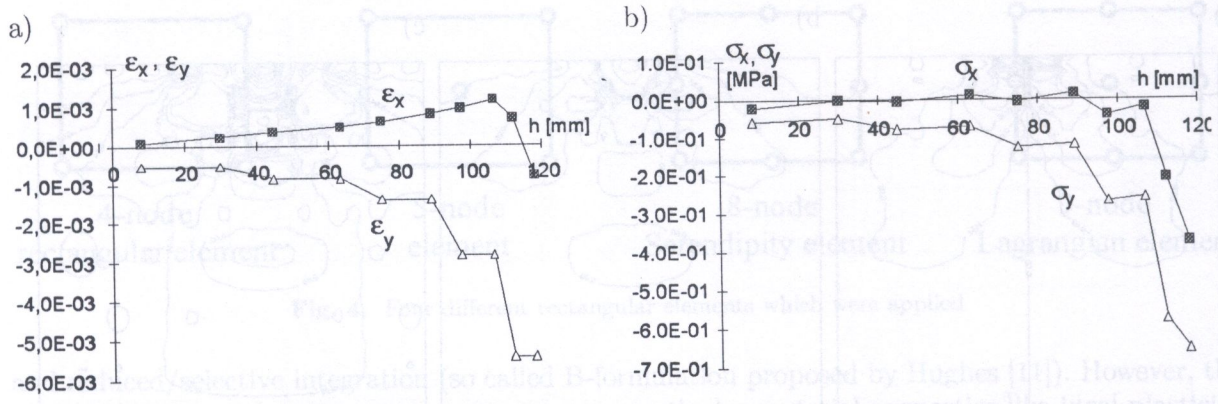

Fig. 7. Distributions of strains and stresses for the column of Gaussian points, which is closest to the central vertical line using the 4-node element: a) horizontal ε_x and vertical ε_y strains, b) horizontal σ_x and vertical σ_y stresses

would not exhibit oscillatory distribution of horizontal stress σ_x, the distribution of vertical stress σ_y would have the layered structure again.

As it was presented in this chapter, the four-node element applied to obtain the solution of the boundary value problem considered, results in the unrealistic, layered stress distributions. Those distributions are strongly related to the horizontal mesh structure and do not depend on the vertical mesh size, the number of integral points, the level of loading force, boundary conditions and elastic constants of the material layer.

2.1.2. 8-node element

Let us consider the boundary value problem presented in Fig. 1a using the 8-node Serendipity element with four and nine integration points respectively. As it was shown in Fig. 8 the distribution of horizontal stress σ_x, does not obey layered structure neither for four nor for nine Gaussian points.

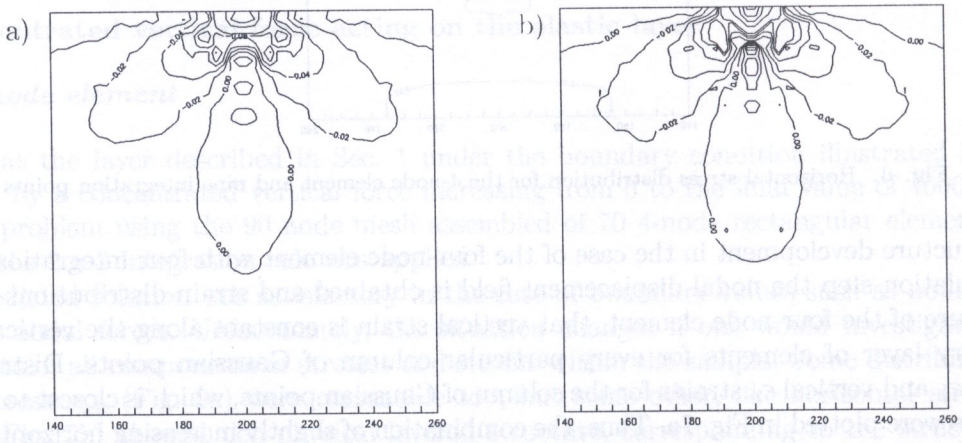

Fig. 8. Horizontal stress distribution for the 8-node element: a) four integration points, b) nine integration points

In the case of the 8-node element the vertical strain changes along the vertical direction within each layer of elements and the stress distributions do not exhibit oscillatory character, like it was in the case of 4-node element. Distributions of horizontal ε_x and vertical ε_y strains and horizontal σ_x and vertical σ_y stresses for the column of integration points, which is closest to the central vertical line was plotted in Figs. 9a and 9b respectively. Those figures should be compared with Fig. 7, obtained for the 4-node element.

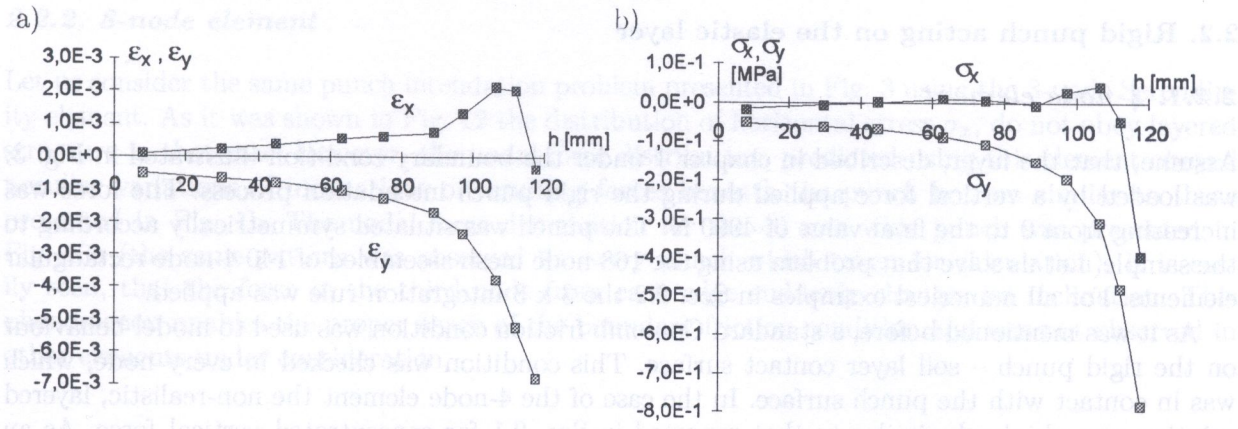

Fig. 9. Distributions of strains and stresses for the column of Gaussian points, which is closest to the central vertical line using the 8-node element: a) horizontal ε_x and vertical ε_y strains, b) horizontal σ_x and vertical σ_y stresses

However, some problems with applicability of 8-node elements occur when the boundary value problem with friction is considered (Fig. 1b).

2.1.3. 9-node element

Let us consider the same boundary value problem using the 9-node Lagrange element: again with four and nine integration points. In the case of four integration points the well known hour-glass mode was observed (Fig. 10a). For nine integration points the obtained solution was smooth and had no peculiar distributions (Fig. 10b). It was concluded to be a proper one for the boundary value problem considered.

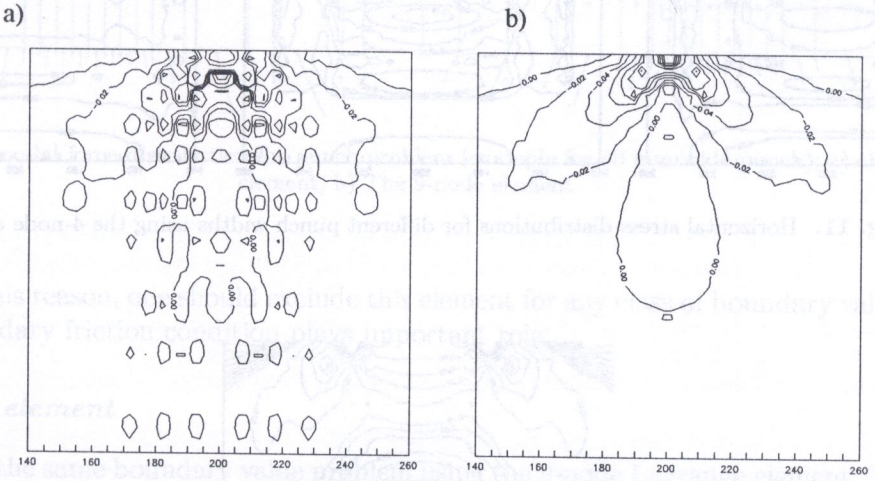

Fig. 10. Horizontal stress distribution for the 9-node element: a) four integration points - hour-glass mode, b) nine integration points

2.1.4. 5-node element

Let us consider again the same boundary value problem using the 5-node element developed as a simplification of the 9-node Lagrangian element. Unfortunately, the obtained solution obeys layered structure, similar to the structure observed for the 4-node element (Fig.5). Thus the application of the 5-node element do not help with the problem discussed.

2.2. Rigid punch acting on the elastic layer

2.2.1. 4-node element

Assume, that the layer, described in chapter 1 under the boundary condition illustrated in Fig. 3. was loaded by a vertical force applied during the rigid punch intendation process. The force was increasing from 0 to the final value of 4000 N. The punch was situated symmetrically according to the sample. Let us solve that problem using the 168-node mesh assembled of 140 4-node rectangular elements. For all numerical examples in Sec. 2.2 the 3 x 3 integration rule was applied.

As it was mentioned before, a standard Coulomb friction condition was used to model behaviour on the rigid punch – soil layer contact surface. This condition was checked in every node, which was in contact with the punch surface. In the case of the 4-node element the non-realistic, layered solution was obtained, similar to that reported in Sec. 2.1 for concentrated vertical force. As an example, the horizontal stress σ_x distributions were shown in Fig. 11 for different punch width and the same friction coefficient μ equal to 20°. In the case of relatively wide punch (Fig. 11c) the layered structure is well observed in zones beneath punch edges, whereas beneath the central part of the punch the distribution tends to be more realistic (compare with Fig. 12). It is worth to add, that the predicted nodal force and nodal displacement solution was pretty good for each punch width, and one could be cheated by it at the first glance. Similar solutions were obtained for the 5-node element.

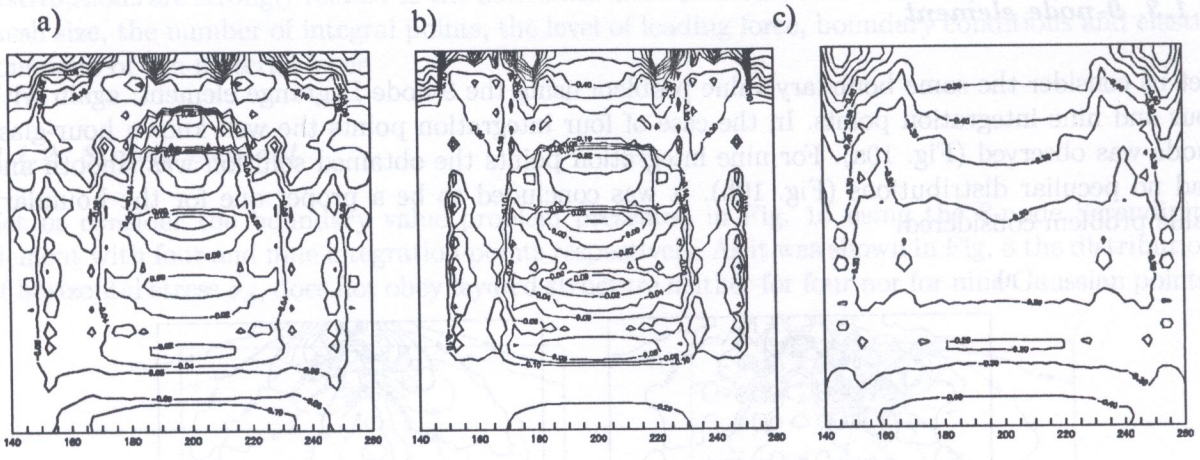

Fig. 11. Horizontal stress distributions for different punch widths using the 4-node element

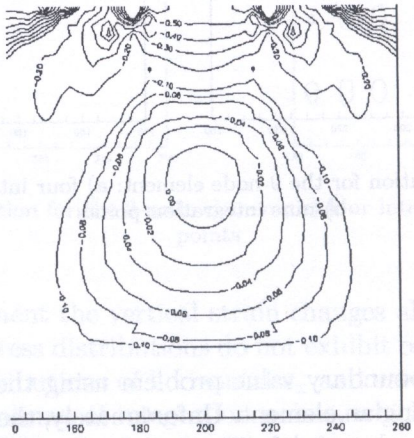

Fig. 12. Horizontal stress distribution for punch problem using 8-node element

2.2.2. 8-node element

Let us consider the same punch intendation problem presented in Fig. 3 using the 8-node Serendipity element. As it was shown in Fig. 12 the distribution of horizontal stress σ_x, do not obey layered structure in that case. However, the nodal force distribution, predicted using this element obeyed peculiar variations of inclinations of resulting forces beneath the punch bottom similar to those presented in Fig. 1b. The nodal force distribution for the 40 mm wide punch was presented in Fig. 13a (the same pattern was observed for every punch width taken for calculation). It is easily seen, that the force in the third node from each edge suddenly changes its inclination. This phenomenon unables the proper usage of the boundary friction condition and was not observed in other elements under consideration.

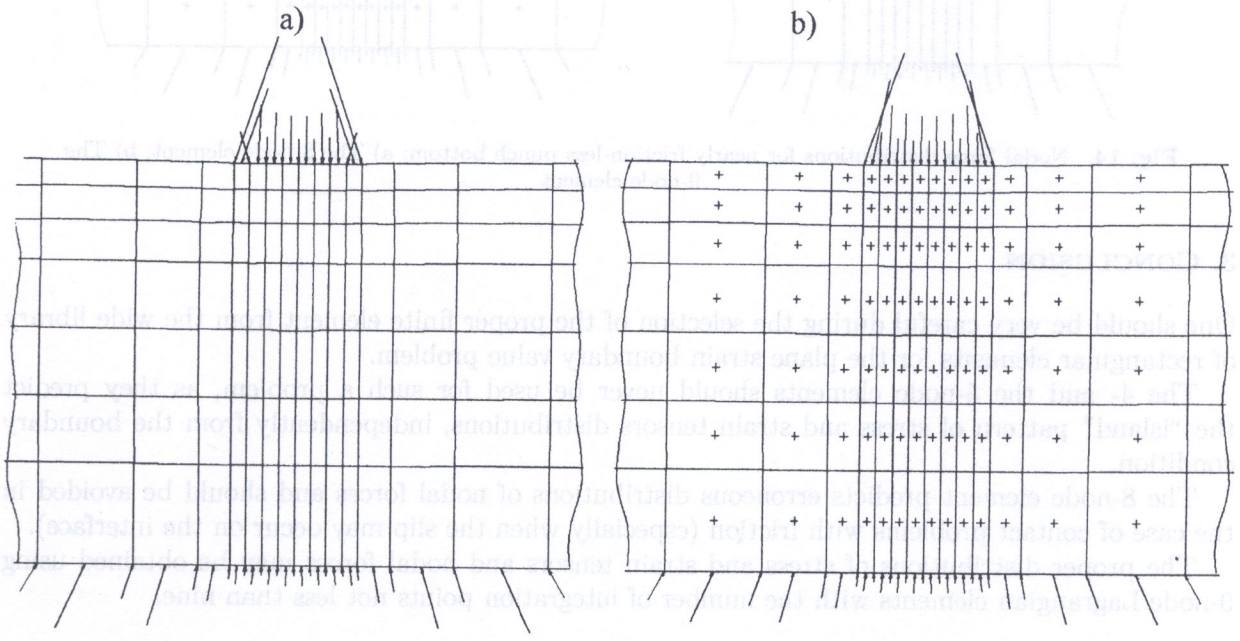

Fig. 13. The nodal force distribution for punch problem (example for 40 mm wide punch); a) the 8-node element, b) The 9-node element

Because of this reason, one should exclude this element for any class of boundary value problems, where the boundary friction condition plays important role.

2.2.3. 9-node element

Let us consider the same boundary value problem using the 9-node Lagrange element. The obtained solution was smooth and had no peculiar distributions (similar to those obtained for the 8-node element). In Fig. 13b the nodal force distribution for the 40 mm wide punch was presented. No abrupt changes of nodal force inclinations were observed.

Similarly like for the concentrated force problem, it was concluded, that the 9-node element with nine integration points was the proper one for the boundary value problem considered.

For additional verification of the boundary friction condition additional calculations were performed for the 8-node and the 9-node elements for friction coefficient μ equal to 2° (nearly frictionless bottom). Their results were shown in Fig. 14a and 14b respectively (compare with Fig. 13a and Fig. 13b). Even for the 8-node element no abrupt changes of nodal force inclinations were observed.

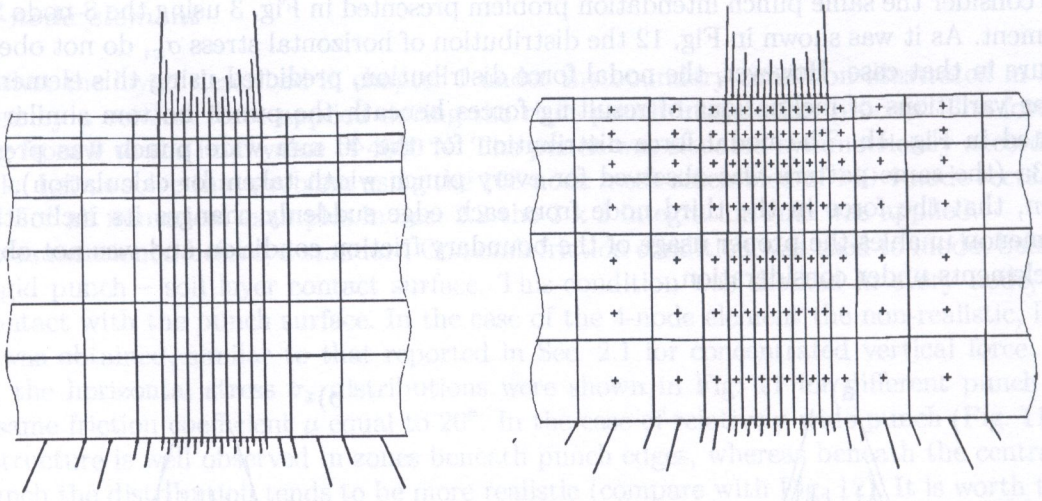

Fig. 14. Nodal force distributions for nearly friction-less punch bottom: a) The 8-node element, b) The 9-node element

3. Conclusion

One should be very careful during the selection of the proper finite element from the wide library of rectangular elements for the plane strain boundary value problem.

The 4- and the 5-node elements should never be used for such a problem, as they predict the "island" pattern of stress and strain tensors distributions, independently from the boundary condition.

The 8-node element predicts erroneous distributions of nodal forces and should be avoided in the case of contact problems with friction (especially when the slip may occur on the interface).

The proper distributions of stress and strain tensors and nodal forces may be obtained using 9-node Lagrangian elements with the number of integration points not less than nine.

References

[1] A. Jarzębowski and Z. Mróz. A constitutive model for sands and its application to monotonic and cyclic loading. *Proc. Constitutive Equations for Granular Non-Cohesive Soils*, Saada and Bianchini (eds.), Balkema, Rotterdam, 307-323, 1988.

[2] A. Jarzębowski and J. Maciejewski. Compaction of a cohesive soil layer under a rigid roll experiment and numerical prediction. *XIX-th ICTAM*, Kyoto, Japan, 25-31 August 1996.

[3] E. Hinton and D.R.J. Owen. *An Introduction to Finite Element Computations*. Pineridge Press Limited, Swansea, 1979.

[4] O.C. Zienkiewicz and R.L. Taylor. *The Finite Element Method*. 4-th edition, Mc Graw-Hill, New Jersey, 1989.

[5] J.T. Oden and J.N. Reddy. *An Introduction to the Mathematical Theory of Finite Elements*. John Wiley and Sons, New York, 1976.

[6] S.W. Sloan and M.F. Randolph. Numerical prediction of collapse loads using finite element methods. *Int. J. Num. Anal. Meth. Geom.*, **6**: 47–76, 1982.

[7] K.J. Bathe and E. Wilson. *Numerical Methods in Finite Element Analysis*. Prentice-Hall, Inc., Englewood Cliffs, New Jersey, 1976.

[8] R.D. Cook, D.S. Malkus and M.E. Plesha. *Concepts and Applications of Finite Element Analysis*. 3-rd edition, John Wiley and Sons, Inc., New York, 1989.

[9] T.J.R. Hughes. *The Finite Element Method*. Prentice-Hall, Inc., Englewood Cliffs, New Jersey, 1987.

[10] R. de Borst A.E. Groen. Element performance in soil and rock plasticity. *Numerical Methods in Geomechancs-NUMOG V*, Pande and Pietruszczak (eds.), Balkema, Rotterdam, 411–416, 1995.

[11] T.J.R. Hughes. Generalization of Selective Integration Procedures to Anisotropic and Nonlinear Media. *Int. J. Num. Meth.Eng.*, **15**: 1413–1418, 1980.

[12] E.L. Wilson, R.L. Taylor, W.P. Doherty J. Ghaboussi. Incompatible Displacement Modes, in Numerical and Computer Models. In: *Structural Mechanics*. Fenves, Perrone, Robinson and Schnobrich (eds.), Academic Press, New York, 43–57, 1973.

[13] R.L. Taylor, P.J. Beresford and E.l. Wilson. A Nonconforming Element for Stress Analysis. *Int. J. Num. Meth. Eng.*, **10**: 6, 1211–1219, 1976.